



Published in final edited form as:

*Prog Polym Sci.* 2007 August 1; 32(8-9): 838–857. doi:10.1016/j.progpolymsci.2007.05.011.

## Emerging Applications of Polymersomes in Delivery: from Molecular Dynamics to Shrinkage of Tumors

Dennis E. Discher<sup>1</sup>, Vanessa Ortiz<sup>2</sup>, Goundla Srinivas<sup>2</sup>, Michael L. Klein<sup>2</sup>, Younghoon Kim<sup>1</sup>, David Christian<sup>1</sup>, Shenshen Cai<sup>1</sup>, Peter Photos<sup>1</sup>, and Fariyal Ahmed<sup>1,\*</sup>

<sup>1</sup>NanoBio Polymers Lab, University of Pennsylvania, Philadelphia, Pennsylvania 19104

<sup>2</sup>Center for Molecular Modeling-Dept. of Chemistry, University of Pennsylvania, Philadelphia, Pennsylvania 19104

### Abstract

Polymersomes are self-assembled shells of amphiphilic block copolymers that are currently being developed by many groups for fundamental insights into the nature of self-assembled states as well as for a variety of potential applications. While recent reviews have highlighted distinctive properties – particularly stability – that are strongly influenced by both copolymer type and polymer molecular weight, here we first review some of the more recent developments in computational molecular dynamics (MD) schemes that lend insight into assembly. We then review polymersome loading, in vivo stealthiness, degradation-based disassembly for controlled release, and even tumor-shrinkage in vivo. Comparisons of polymersomes with viral capsids are shown to encompass and inspire many aspects of current designs.

### Keywords

liposomes; amphiphile; block copolymers; nanoparticles; controlled release

## 1. INTRODUCTION

Viral capsids are perhaps the prototypical ‘supramolecular assemblies for hollow structures’, which is the inspired theme of this collection of reviews that includes the review here on ‘polymersomes’. Viral capsids self-assemble from polypeptides and serve to contain the virus’ genome, thereby protecting the nucleic acid from degradation. The robust capsid shells also integrate delivery mechanisms with viral targeting and controlled release. Polymersomes are likewise self-assembled – but from synthetic polymers rather than peptide-based polymers, and these synthetic shells are now being engineered to perform some of the same functions as robust viral capsids, namely to carry, protect, target, and release actives (drugs, nucleic acids, and dyes).

For both viruses and now polymersomes, structurally detailed models of assembly and disassembly are emerging and should provide deeper insight into energetics as well as

---

© 2007 Elsevier Ltd. All rights reserved.

discher@seas.upenn.edu

\* current address: CBRI, Harvard Medical School

**Publisher's Disclaimer:** This is a PDF file of an unedited manuscript that has been accepted for publication. As a service to our customers we are providing this early version of the manuscript. The manuscript will undergo copyediting, typesetting, and review of the resulting proof before it is published in its final citable form. Please note that during the production process errors may be discovered which could affect the content, and all legal disclaimers that apply to the journal pertain.

mechanisms of loading and delivery of nucleic acid or drug. Both modeling and delivery aspects of polymersomes are our dual focus in this integrated review. As recently summarized [1], the selection of synthetic polymer(s) and especially the choice of molecular weight ( $M$ ) of the polymers used for polymersomes are critical since these impart these vesicular shells with a broad range of tunable carrier properties.

Amphiphilicity is exploited for polymer vesicle assembly. Nature's own vesicle-forming amphiphiles are lipids that almost always possess  $M < 1$  kDa (Fig. 1A), whereas vesicle-forming polymers are invariably much larger. The copolymers used have at least one hydrophilic fraction or 'block' linked to a hydrophobic block that is as large or larger. Either type of amphiphile, lipid or block copolymer, if made with suitable amphiphilic proportions, can self-direct its collective assembly into closed vesicles upon hydration of a cast film. Heat and sometimes co-solvent are needed to fluidize the films, but the hydrophobic blocks of each molecule have an intrinsic tendency to aggregate and minimize direct exposure to water while the more hydrophilic blocks form inner and outer brushes that are well-hydrated and define or delimit the inner and outer interfaces of a typical bilayer vesicle.

As derived from nature, lipids tend to be biocompatible, which has partially motivated broad efforts to develop liposomes into drug carriers over the last several decades. However, liposomes lack controlled release mechanisms among a number of other pharmacokinetic limitations. These include a limited circulation in the body of hours or less, which minimizes the likelihood of delivering drug to an intended target site. This shortcoming was first addressed about two decades ago by adding a hydrated polymer layer on the liposome that some would describe as a mimic of the carbohydrate coat or glycocalyx on cell membranes. This is most commonly achieved through attachment of biocompatible PEG, polyethylene glycol (or PEO, polyethylene oxide) to a small fraction (5-10%) of the lipid headgroups, as reviewed further below. Since then, a range of PEO based diblock copolymers have emerged that altogether eliminate the need for lipid in vesicle formation. Promising biocompatible copolymers include PEO plus degradable chains, such as PEO-poly(lactic acid) (PEO-PLA) and PEO-poly( $\epsilon$ -caprolactone) (PEO-PCL), which are not only being widely synthesized to make polymersomes but are also now commercially available off-the-shelf or custom synthesized, broadening accessibility for a new generation of researchers.

Cells are no doubt capable of synthesizing super-amphiphilic compounds similar in form to the diblocks described here, but the low  $M$  of natural lipids imparts biomembranes with lateral fluidity and other "soft" properties [1] that are no doubt conducive to various cellular processes (endocytosis, cell division, receptor clustering, etc.). Fluidity does not seem necessary for viral capsids but genome protection is essential, and so nature has switched to the lock-and-key assembly of proteins. Capsid proteins are polypeptides with a typical  $M$  in the range of 10-20 kDa or higher, corresponding to polymerization numbers of approximately 100-200 amino acids or more, and these proteins self-assemble into hollow carriers that are more shell-like and tough [2]. With polymersomes, the copolymers extend to this range of  $M$  (as a number-average  $M_n$ ), but the copolymers assemble more like lipids than in a lock and key fashion.

A first goal of this brief review is to describe the insights provided by modern computational methodologies into the nature of a small subset of the first generation PEO-based copolymer assemblies. A second goal is to provide an update of the loading and delivery applications that are emerging with these hollow structures. The results to date suggest fertile ground for mimicry of viral capsids as well as some promise for a wide variety of tailored applications.

## 2. MOLECULAR DYNAMICS OF POLYMERSOME ASSEMBLY

Copolymers that are composed of at least one hydrophilic block and one strongly hydrophobic block have been widely seen in experiment to self assemble in water to yield a variety of morphologies. The two driving forces for organization are the difference in solubility of the blocks and the constraint imposed by the chemical linkage between the blocks, which together influence the geometry of the assembly. Polymers used for the hydrophobic block(s) are already numerous and include inert polyethylene (PEE) and its de-hydrogenated polybutadiene precursors (1,2- or else 1,4- PBD), polystyrene (PS), polydimethylsiloxane (PDMS), and the degradable PLA and PCL. Hydrophilic blocks have included negatively-charged polyacrylic acid (PAA), crosslinkable polymethyloxazoline (PMOXA), but probably the most common is neutral PEO, which is widely used for bio-applications as mentioned already for liposomes. Explicit computer simulations of such polymeric systems can be a challenge because of the high molecular weights intrinsic to polymers as well as the need for explicit water to capture hydrophobic effects and large system sizes. Nonetheless, the challenges across various length scales (Fig. 1A-D) are beginning to be met as reviewed here.

Classically, assembly geometry is dictated by block proportions described by a packing parameter  $p = v / a l_c$ , in which  $v$  is the volume of the densely-packed hydrophobic segment,  $a$  is the effective cross-sectional area of the hydrophilic group, and  $l_c$  is the chain length of the hydrophobic block normal to the interface [3]. Based on simple geometric ideas of core volume versus surface area, one can show that  $p < 1/3$  is characteristic of spherical micelles; whereas  $1/3 < p < 1/2$  yields cylindrical micelles; and  $1/2 < p < 1$  corresponds to vesicles. Flat lamellae form for  $p = 1$ , and inverted structures are expected for  $p > 1$ . These trends are well established for small surfactants and lipids and are generally followed also for amphiphilic block copolymers, although it is generally preferred to characterize diblocks by the more synthetically accessible hydrophilic block fraction  $f$  ( $0 < f < 1$ ) rather than the core packing parameter  $p$ . Based on summaries below of morphology results from both simulation and experiment for various amphiphilic copolymers, an excellent correlation is provided by the equation:

$$f \approx e^{-p/\beta} \quad (\beta=0.66)$$

From a synthetic point of view, this correlation indicates that vesicles as target structures are in the higher order terms so that a *non-linear*, exponential series of  $f$  would be more appropriate to make (rather than  $f = 0.2, 0.3, 0.4 \dots$ ). Any deeper thermodynamic meaning to the correlation above is presently unclear.

Since polydispersity of the chains (in both  $f$  and  $M$ ) is an intrinsic feature of synthetic polymers in addition to high degrees of polymerization, it has further been reported that vesicles formed by diblock copolymers are thermodynamically stabilized by segregation of a sub-population of chains to the inner or outer leaflet of the membrane based on their hydrophilic-to-hydrophobic block length ratio [4]. Computer simulations can in principle help elucidate such heterogeneity and morphological determinants, but they have yet to be applied to this particular question. While many other aspects of the computational approaches have been recently highlighted [5], we provide a brief overview of simulations and results in the context of experimental progress in delivery.

### 2.1 Detailed Computer Modeling and Simulation

In atomistic modeling, all of the atoms in the system are explicitly represented and the interactions are usually quantified by potentials for chemical bonds, bond angles, dihedral

angle torsions, electrostatics, and non-bonded (van der Waals) interactions. The non-bonded interactions are often described using pairwise Lennard-Jones potentials, bonds and angles are described by harmonic potentials, torsions are usually represented with a truncated Fourier series, and electrostatics by Coulomb potentials. All of these potentials are conservative, which means the forces are obtained from gradients in the potentials. Two widely used parameter sets are CHARMM [6] and Amber [7], but these are both optimized for biological systems near 300 K and do not treat certain functional groups needed to model synthetic polymers. OPLS [8] is perhaps a more appropriate choice for the simulation of block copolymer systems because it was built for modeling organic molecules.

Given the length- and time-scale limitations of atomistic simulations, very few studies had been done on block copolymer systems using atomistic molecular dynamics (AMD) before the 1990's, with the systems usually consisting of a single polymer chain in implicit solvent. A few computational studies have focused on the behavior of polyethylene oxide (PEO) because of the multiple biological applications that seem to reflect PEO's unique solution properties in water. This is due mainly to its structural similarity with water, strong hydrogen bonding to the ether oxygen atoms, and high flexibility and mobility in aqueous solution. Anderson and Wilson [9] described the organization of PEO based copolymers at the air/water interface. They used AMD trajectories to construct density profiles that could be directly compared to experimental neutron reflectivity data over a wide range of polymer surface concentrations. Previously, experimental neutron reflectivity data for such systems could only be deduced through the fitting of structural parameters (layer composition and thickness). The simulation gave a reflectivity profile in excellent agreement with experiments at low surface concentrations, while agreement at high concentrations was significantly better than in a previous model that neglected water [10]. Also, as the surface concentration of the molecule was increased, the authors were able to observe a transition of the PEO block from a pancake conformation to the hydrated brush conformation. In general, computer simulations at the atomistic level are necessary to gain insight into detailed interactions such as hydrogen bonding, polymer-solvent interactions and specific conformational effects (e.g. *cis/trans* isomerization). However, another use for AMD simulations can be to provide inter- and intra-molecular data, useful as input in the parameterization of coarse grain models.

A wide variety of coarse-grain (CG) models have been developed to simulate block copolymer systems on length scales that are far larger than can be accessed using atomistic models. Coarse grain models involve representing a group of atoms by a single sphere. In view of this simplification, the full chemical details of the molecules cannot be retained. However, effective interactions among the spheres can be chosen to mimic some key features of the real polymer chain. The representation of a collection of atoms, with considerable internal flexibility, by a single site leads to softer interaction potentials between sites which also permit large time-steps to be used. Since the number of particles is reduced by at least an order of magnitude, and since the interactions are simpler and more computationally efficient, CG models have become a popular tool in the polymer community over the last two decades. In 1996, Semenov published one of the first papers on self assembly of block copolymer *A-B* amphiphiles [11]. In this study, the polymers were represented as chains of either 4 or 8 units (each representing statistical segments of the real polymer molecule rather than monomers). One of the end units was *B*-type (hydrophobic) while the rest of the molecule was *A*-type (hydrophilic), and the chains were immersed in a good solvent for the *A* monomers. At this point, the models used to describe the molecular interactions were rather simple and arbitrary, partly for computational efficiency but also because limited knowledge concerning the corresponding molecular forces was available. These models allowed for an explicit connection between the molecular and continuum descriptions. Such a connection was perhaps first demonstrated by Goetz, Gompper, and

Lipowsky [12] for mechanical properties of membranes, including determinations of the stretching elasticity and the bending rigidity that agreed reasonably well with experiment. Nonetheless, even with the increase in efficiency over atomistic models, severe limitations on the sizes and timescales accessible still exist, and therefore early studies focused on block copolymers were mostly reported for ‘short’ chains with block lengths from 2 to about 30.

Increasing levels of detail in the models began to be incorporated in the work of various groups by around 2001 or 2002. Model parameters (interaction energy, force constant, radius of interaction, mass, volume) were still chosen in a somewhat arbitrary way, but added details included explicit water [13-15] and bending potentials to account for three-body interactions [15]. More capable computers also enabled an increase in the number of particles in the systems (although chain lengths remained short) and, as a consequence, other types of morphologies apart from the spherical micelles, such as worms and vesicles, could be observed. Maiti and co-workers [15] observed different morphologies in the self-assembly of supramolecular aggregates of model surfactant oligomers in an aqueous medium by using a CG model with NPT MD simulations. They studied the effect of the degree of oligomerization  $m$  (in hydrophobic tails) and surfactant concentration  $c$  on the nature of the self-assembly, as well as on the micelle size distribution. They reported a decrease in the critical micelle concentration  $cmc$  with increasing  $m$ . When increasing  $c$ , both two-tail and three-tail surfactant systems exhibited a transition from spherical micelles to cylindrical micelles. With further increase in  $c$ , these cylindrical micelles transformed into extremely long “wormlike” or “threadlike” micelles, but no true vesicles were seen.

In 2004, the first in a series of papers began to appear [16-19] in which a coarse-grain molecular dynamics model for polyethyleneoxide-polyethylene (PEO-PEE) was developed and applied to compute morphologies and physical properties of assemblies in water. The model was built to replicate a collection of data obtained from both experimental and atomistic computer simulation methods [16]. Each CG polymer site represents one monomer (3 heavy atoms on average), and a CG water site represents 3 H<sub>2</sub>O's. The mass of each site was determined from its constituent atoms, while the interaction energies ( $\epsilon$ 's) and radii of interaction ( $\sigma$ 's) were chosen to replicate the experimental bulk density and surface tension of the species, respectively. Also, the intra-molecular structure of the polymers was incorporated by adding harmonic bonds and bends for which the force constants ( $k_x$ 's and  $k_\theta$ 's) and equilibrium values ( $x_\theta$ 's and  $\theta_\theta$ 's) were chosen to replicate the first and second moments of the bond and angle distributions obtained from atomistic molecular dynamics simulations (Fig. 1A).

In CG water, the model replicated the experimentally observed phase behavior of hydrated PEO-PEE diblock copolymers. With hydrophilic-to-hydrophobic block length ratios ( $f_{EO}$ ) ranging from about 0.3 to 0.7, initially random configurations of diblock copolymers in water self assembled respectively into either a bilayer (Fig. 1B), a cylindrical micelle, or a spherical micelle (Table 1) [17]. Also, simulations done on the triblock copolymer PEO-PEE-PEO in water have shown assembly into “tube”-like structures in which 38% of the molecules appear arranged in a linear configuration spanning the membrane of the tube, while the rest of the chains acquired a hairpin configuration [19].

The CG model has been used to study the effects of block length on different physical properties of the bilayer configuration such as the area elastic modulus, the scaling of the hydrophobic core thickness and the lateral chain mobility [17]. As elaborated below, the scaling of the hydrophobic core thickness with hydrophobic block length in the bilayer configuration agrees with experimental results reported [20] on bilayers in the same block length regime that was accessible to simulation. The simulation data was also used to calculate the absolute value of the bilayer's area elastic modulus, and it was found to be

independent of block length, in good agreement with the experiments. Additionally, the experimental diffusivity of the diblocks was compared with data collected from the simulations on the extent of overlap and entanglement between the two leaflets of the bilayer, suggesting a crossover in diffusivity from the linear Rouse regime at low  $M$  to a regime seemingly dominated by entanglements at high  $M$ . Deeper insight into mobility processes, such as the expected mechanism of activated reptation, was limited by computational time. Simpler algorithms have therefore been developed for studies of larger systems and longer times.

Dissipative Particle Dynamics (DPD) is similar to the molecular dynamics above in its use of CG models except that dissipative and random forces act between particles in addition to the usual conservative interactions. While intended to mimic the influences of neglected degrees of freedom, the dissipative and random forces also collectively serve as a thermostat. The atomistic-to-coarse grain mapping is usually similar to that in MD and MC. All of the forces employed in typical DPD simulations conserve momentum and hydrodynamic interactions are correctly represented. Warren [21] recently reviewed the technique. Many improvements have been implemented within the DPD framework in the last few years such as modifications in the integrators to eliminate the sensitivity to time-step size [22], and extension beyond the usual constant volume ensemble to a constant pressure ensemble [23].

By using dissipative particle dynamics (DPD), Yamamoto and Hyodo could capture some of the mechanisms for spontaneous vesicle formation of amphiphilic molecules in aqueous solution [14]. In the DPD simulation, starting from both a randomly dispersed system and a bilayer structure of the amphiphile, spontaneous vesicle formation was observed through the intermediate state of an oblate micelle or a bilayer membrane. The mechanism consisted of fluctuations in the membrane that encapsulates water particles with eventual sealing to form a vesicle. They tracked the hydrophobic interaction energy between the amphiphile and water as a function of time and observed a decrease in this quantity as the vesicle formed. They also compared timescales for vesicle formation for single-tail and two-tail amphiphiles, finding faster kinetics for the two-tailed amphiphiles than for the single-tailed ones. The same method was also applied to study the budding and fission dynamics of two component vesicles [24]. By changing the strength of the interactions between the amphiphiles forming the vesicle, it was possible to make them segregate into domains (rafts) within the membrane. These domains caused deformations in the membrane that, when large enough, caused fission of the vesicle into two or more smaller vesicles formed from either one of the amphiphile types.

The DPD framework has also been used with a new coarse-grain model for PEO-PEE by the groups of Klein and Discher in collaboration with Lipowsky's group [25]. Due to the simpler interactions, DPD allows an increase in system size sufficient to simulate entire vesicles while still maintaining the diblock molecular weight within the experimental range (Fig. 1C). The PEO-PEE model was built, as before, by matching experimental surface tension and density data together with atomistic MD intra-molecular structural information. Building the model required the introduction of a density-based atomistic-to-coarse-grain mapping in order to obtain a physically realistic description of the system. After introducing these changes to the DPD framework, the resulting DPD model for PEO-PEE gave values for the membrane area elastic modulus and the power-law scaling of the hydrophobic core thickness that were again in excellent agreement with the experimental values. In addition, mechanisms of vesicle content release via vesicle rupture induced by osmotic swelling were explored with this model (Fig. 1D).

### 3. POLYMERSOME STRUCTURE, STABILITY, AND CONTROLLED RUPTURE

Experimentally, both  $\text{PEO}_m\text{-PEE}_n$  and its unsaturated pre-cursor  $\text{PEO}_m\text{-PBD}_n$  can be made with suitable  $m$  and  $n$  to self-direct their assembly under a variety of aqueous conditions into unilamellar polymersomes (Fig. 1E) [20,26]. Such images not only allow for direct measurements of the thickness  $d$  of the hydrophobic core of each membrane, which reflects the densely self-assembled PEE or PBD (unstained), but they also consistently show a revealing gap between the closely packed vesicles. Since the vesicles are squeezed within a film for the imaging and because the minimum gap consistently approximates  $d$ , it seems very likely that this gap is filled with a hydrated brush of PEO and gives the indicated  $d_{\text{brush}}$ . A few dashed red lines indicate the dividing line between the brushes of adjacent vesicles. Both  $d$  and  $d_{\text{brush}}$  are seen to increase with copolymer  $M$ . The scaling of  $d$  is discussed below in the context of simple predictions, while the effects of the thickening  $d_{\text{brush}}$  are described below in a different context of protein deposition in applications of polymersomes to biology.

As with liposomes, polymersomes can be sonicated or extruded through nano-porous filters to obtain nano-polymersomes that are approximately the size of viruses and can be labeled with hydrophobic or hydrophilic fluorescent dyes (Fig. 1F, left) for tracking by fluorescence microscopy in solutions, cell cultures, or animals. Pure systems can also of course be sized by dynamic light scattering for studies of stability. The right-side of figure 1F demonstrates the stability of PEO-PBD vesicles with no change in vesicle size over a month, which contrasts with the rupture and breakdown over days of degradable PEO-PLA based vesicles that are described further below [27-29].

With micron-sized polymersomes that are amenable to single vesicle manipulation, physical properties of the polymersome membranes have been measured by methods common in liposome research and cell biophysics. As reviewed elsewhere [30,31], such studies demonstrate the thick-walled vesicles are electromechanically tough, have low permeability relative to lipid membranes [32], possess a viscous shell-like character [33], and exhibit elastic properties that are set by the interfacial tension between the two blocks and again  $d$ , at least for bending.

Copolymers that have yielded polymersomes in our own studies have thusfar had number-average  $M$ 's in the range of ~2-20 kDa, yielding respective core thicknesses of  $d \approx 8\text{-}21$  nm [20,34]. In comparison, lipid membranes have a far more limited range of  $d \approx 3\text{-}5$  nm, which is clearly compatible with insertion of the many integral membrane proteins in cells. Scaling of  $d$  with copolymer  $M$  – or at least the hydrophobic block's molecular weight  $M_h$  – was shown in experiments on PEO-PBD and PEO-PEE polymersomes and also confirmed by a CG molecular dynamics simulation [17] to fit:

$$d \sim M_h^b \quad (b \cong 0.55)$$

Classical strong segregation theory of Semenov would predict  $b \cong 0.67$  and has been reported by Battaglia and Ryan with a more weakly segregating copolymer system that yields thinner membranes [35]. The simple free energy expression (per copolymer) of Semenov simply adds interfacial energy due to surface tension  $\gamma$  to a chain elasticity term with no other terms of importance:

$$F \cong \gamma a + k_B T \frac{d^2}{\sigma^2} M + \text{additional terms}$$

where  $d = M \sigma^3$  due to bulk incompressibility. While minimizing  $F(d)$  yields

$$d \sim \left( \gamma \delta^5 / k_B T \right)^{1/3} M^{2/3}$$

simulation has shown that, for low  $M$  systems (of PEO-PEE), the polymer bilayers have a clear midplane of low density, which is known as the “methyl trough” for lipid bilayers, whereas high  $M$  copolymers show two bilayers that interdigitate or “melt” together into a single thick shell of homogeneous density. This additional mixing entropy (in the ‘additional terms’ above) would tend to suppress strong scaling of the thickness with  $M$ . Regardless of small differences in scaling, polymersome membranes have provided a novel opportunity to study membrane properties as a function of membrane thickness  $d$ . Indeed, as cited already, properties such as the membrane bending rigidity ( $K_b$ ) scale with  $d$  ( $K_b \sim d^2$ ) as does electromechanical stability.

Stable containment and protection of nucleic acid by viruses have evolved over eons (and continue to evolve) for release at a suitable time and place. Disassembly of a viral capsid is sometimes triggered at low pH and is often sensitive to environmental variables such as temperature. In comparison, many if not all conventional liposome systems have proven to be both inherently leaky [36] and short-lived, especially in the circulation [37]. In efforts to integrate mechanisms of controlled release in liposomes, PEG-lipids have been made to play dual roles as liposome stabilizers that also, upon exposure to an environmental stimulus, effectively destabilize the carrier membrane viatholytic [38] or hydrolytic [39,40] cleavage. The precept for such efforts and also for similar developments with block copolymers is that for a simple amphiphile, a time-average molecular shape in the form of a cylinder, wedge, or cone dictates aggregate curvature and thus whether membrane, cylindrical, or spherical morphologies are thermodynamically preferred [3,41]. This average molecular shape is most simply a reflection of the hydrophilic volume (or mass) fraction  $f$ . Importantly, with reactive copolymers, this critical determinant of assembled morphology can be made to change.

Block copolymers of PEO-PLA (equivalent to PEG-PLA) have been known in the past to make micelles and nanoparticles [42,43] and have been of great interest because PLA's susceptibility to hydrolytic biodegradation can be exploited for drug release [44]. However, vesicles made from PEG-PLA had not been reported years ago probably because of the narrow range of  $f$  required for a stable vesicle phase. Indeed, the molecular-scale force balance outlined above allows the design of PEG-block-based copolymers that – in the absence of degradation – form membranes in preference to other structures. Solid-like particles of PEG-PLA had been reported using diblock copolymers with small hydrophilic PEG fractions of  $f < 20\%$  and large  $M$  hydrophobic blocks [42,45], whereas for  $f > 42\%$ , reports have appeared for both worm micelles (up to  $f \sim 50\%$ ) [46,47] and spherical micelles of PEG-PLA [48] and poly(ethylene glycol)-poly(caprolactone) (PEG-PCL) [49]. With  $f \approx 20\text{--}42\%$  for these two types of block copolymers, “loose” micellar architectures had been reported [48], but such a description seems more appropriate for the degraded remnants of vesicles that were characterized [50,51] soon after PEG-polyester vesicles were introduced [30].

Thus, on the basis of the examples above, along with others, one unifying rule (or at least a starting point) for generating polymersomes in water is a phospholipid-like ratio of hydrophilic fraction to total mass:  $f \approx 35\% \pm 10\%$ . A cylindrically shaped molecule that is asymmetric with  $f < 50\%$  presumably reflects the ability of hydration to balance a disproportionately large hydrophobic fraction. Molecules with  $f > 45\%$  can be expected to



form micelles, whereas molecules with  $f < 25\%$  can be expected to form inverted microstructures.

Polyester-based degradable polymersomes have thus far been made from PEGPLA (Fig. 1F, right), PEG-PCL, or other PEG-polyesters and can make mechanically stable vesicles [50-54]. Such vesicles have perhaps been studied most thoroughly as blends with inert PEO-PBD for control over vesicle degradation and content release times. Indeed, the release rates of encapsulated molecules increase linearly with the mole ratio of PEG-PLA [51], and it is visibly clear that mixed membranes are homogenous, as verified by fluorescence microscopy [50].

Although initial investigations of PEG-polyester based systems appear promising, the phase behaviour and biodegradation of the polyester blocks in nano-scale assemblies is potentially complicated by their glassiness or crystallinity. Such states will be influenced by defect densities and additives, particularly cosolvents but also other copolymers and perhaps drugs. Nonetheless, work done thusfar on the PEG-polyester assemblies shows that hydrolysis occurs preferentially at the chain end rather than mid-chain [47], and so a preferred curvature will arise with degraded chains in the membrane, transforming stable bilayer-forming chains into detergent-like copolymers. Such degraded chains with comparatively short hydrophobic blocks will tend to segregate, congregate, and ultimately induce hydrophilic (i.e., PEG-lined) pores. For broadened control, if needed, encapsulant release times can be set through blending inert and degradable chains and can range from hours to weeks.

Molecular scale transitions due to degradation are evident in various physical observations, such as encapsulant release, which decreases with increasing  $M$ . Eventually, the vesicle carriers disintegrate into mixed micellar assemblies – as is evident in both fluorescence microscopy and electron microscopy measurements [55]. Block polyester participation in the bilayer morphology appears strongly dependent on the rate of hydrolysis of the hydrophobic block (e.g., PCL versus PLA), as well as the initial hydrophilic block ratio,  $f$ . Parallel studies with varied polyester hydrophilic/hydrophobic block ratios, hydrophobic chemistry, and different mole-percent blends indicate that polyester chain hydrolysis is indeed the molecular trigger controlling encapsulant release and polymersome carrier destabilization kinetics. A strong dependence of degradation rate on pH is seen [56] as recently quantified for degradation of worm micelles composed of PEO-PCL [47].

Instead of polyester hydrolysis, Hubbell and coworkers [57] have developed oxidation-responsive polymersomes from PEO-(propylene sulphide)-PEO triblock copolymers. The idea is to exploit the oxidative environment present in sites of inflammation as well as within endolysosomes. Studies to date show that exposure to either aqueous  $H_2O_2$  or  $H_2O_2$  generated from a glucose-oxidase/glucose/oxygen system will oxidize the hydrophobic propylene sulphide core and transform it to poly(sulfoxides) and poly(sulfones), which are hydrophilic. Oxidation thus increases  $f$  of the macroamphiphile and thereby destabilizes the vesicle morphology, eventually leading through worm micelles to soluble oxidized copolymer. A more dramatic rupture and release process has been reported by Forster and coworkers using PEO-P2VP based polymersomes that disassemble when the core block is protonated at a low pH typical of bio-acidic environments within internalizing compartments inside cells [58].

#### 4. INTERACTIONS WITH BIOMOLECULES AND CELLS, AND THE BASIS FOR EXTENDED CIRCULATION IN THE BODY

In bio-applications that might exploit the controlled release mechanisms above, carriers such as polymersomes are typically injected intravenously. This exposes otherwise pristine assemblies to a high concentration (5% w/v) of biomolecules in the serum – including a wide range of free and assembled surfactant (lipids, cholesterol, fatty acids, etc.) plus thousands of types of both soluble and surface-active proteins (albumin, immunoglobulin, complement proteins, etc.). Of course, vesicles also contact red blood cells (~40% v/v) and white blood cells plus various tissue cells that include endothelial cells, which line blood vessels, and macrophages and neutrophils, which engulf or phagocytose foreign particles. Some of these transient or sustained interactions with biomolecules and cells have been studied by both experiment and simulation. The results show as reviewed below that (i) the PEG brush is a useful *kinetic* barrier to interaction, and (ii) the thickened cores of polymersomes are soft and penetrable and will admit hydrophobic interactions in combination with chain deformation.

While it is known that slight differences in lipid chain length can cause microphase segregation in membranes, copolymers and lipids appear miscible: a moderate  $M$  triblock copolymer will mix homogeneously with lipids in polymer-lipid composites [59]. Additionally, mixing of lipid membranes with concentrated copolymer micelles – as products of PEG-PLA vesicle breakdown (Fig. 1F, right side) – has been demonstrated with cells [56] and even exploited as elaborated below.

Polymer systems can also, with prudent design and application, open new pathways for the delivery of drugs and mimic in some ways how viruses deliver their nucleic acid. Cationic aggregates are a popular, sometimes toxic, choice of carrier that fosters intracellular delivery through a “proton sponge” effect on cellular vesicles known as endolysosomes that internalize carriers and viruses [60]. However, cationically charged nanoparticles are cleared from circulation within minutes [61]. We have recently attempted to address the problem of endolysosomal escape with the neutral degradable polymersomes discussed above. Under mildly acidic conditions found in these intracellular compartments, PEG-polyester polymersomes degrade 2-3 fold faster than in the neutral extracellular milieu. Hydrolytic rupture generates polymeric micelles and macrosurfactants that can accumulate to high concentrations within the endolysosomes where they integrate and disrupt lipid membranes [56]. Such results might resolve a controversy over escape mechanisms with PEO-PCL micelles [62] since the accumulated data suggest that the lytic time constant  $\tau_{\text{lysis}}$  for PEG-polyester-mediated rupture of lipid membranes scales inversely with hydrophilic fraction  $f$  while scaling directly with  $M$  of the hydrophobic block [1].

Simulations [17] mentioned above in the context of membrane-thickness scaling have been extended to studies of lipid interactions and tend to confirm a lytic tendency with increasing  $f$ . Thus, although self-assembled membranes of copolymer and self-assembled membranes of lipid interact minimally, similar copolymers assembled into spherical micelles will fuse, mix, and porate a lipid membrane. If the micelles are generated by polymersome degradation, the same process applies [56]. Given that the endolysosomal membrane is the cell's last barrier to cytoplasmic entry, the copolymer-mediated poration summarized here is seen to create a new pathway for drug escape and delivery to intracellular targets that include nuclear DNA (for doxorubicin) and microtubules (for taxol).

#### 4.1 Directed studies of protein insertion

Integration of protein channels into thick diblock copolymer membranes was initially realized by Meier and coworkers who exploited their systems for many purposes, including (amazing) viral nano-injection of DNA into polymer vesicles [63-65]. Subsequent studies by Schmidt and coworkers directed at sensor applications demonstrate single channel functionality [66] while Montemagno and coworkers have had the ambition of applying protein-driven energy transduction across polymeric biomembranes [67].

By CG MD methods, a model membrane protein with a cylindrical pore has also been simulated in its insertion into diblock copolymer membranes of different thicknesses (Fig. 2) [19]. The simulations show that chain flexibility, combined with hydrophobic mismatch, has two important consequences on membrane-channel function. First, in the absence of polydisperse chains that might be thought necessary to provide small compatibilizing chains around the channel, copolymer flexibility allows accommodation of comparatively small protein inclusions into membranes of various thickness. Secondly, flexible chains transiently block (water) permeation of the pore through a combination of corona filtration and pore obstruction by chains. Decreased activity of polymersome inserted channels was indeed reported in the early work by Meier and coworkers.

The various studies of protein insertion provide some of the clearest examples of protein interactions with membranes. Active channels are clearly formed, implying maintenance of the folded proteins, and simulations reveal relevant mechanisms. More complicated channel-forming systems consisting of naturally occurring membrane-perforating antimicrobial peptides have also been studied [68]. Pore assembly starts by adsorption of the amphipathic cationic helices to the membranes, with spectroscopic methods demonstrating that adsorption definitively occurs on the neutral, fully PEGylated polymersomes, albeit less efficiently than with liposomes. At higher concentrations of amphipathic peptides, the peptides insert and collect into pores that perforate the hyper-thick polymersome membranes and eventually rupture them. The critical concentrations are again high, but the ~3-5 nm long helices of the peptides are clearly capable of forming pores that span across membrane cores of  $d = 9-15$  nm. The results show that antimicrobial peptides should be viewed as genetically encoded but otherwise fairly generic surfactants rather than targeted poration complexes with exclusive specificity for microbial membranes composed of specific lipids. More generally, the results also show that proteins will permeate the brushy PEG corona and interact strongly with the copolymer membranes regardless of their increased thickness.

#### 4.2 PEG imparts imperfect stealth in blood even at 100% PEGylation

PEG was originally conjugated to lipids to mimic the cell-protective glycocalyx and enhance the biocompatibility of liposomes [69]. Structurally, the behavior of lipids when conjugated at the hydrophilic head group with PEG chains is no different than with the copolymers above. With doxorubicin-loaded liposomes known commercially as DOXIL® and many related liposome systems, the typical PEG chains used ( $M \approx 2000-5000$  Da [36]) lead to a conically shaped amphiphile with  $f \gg 50\%$ . This is distinct in form from cylindrically shaped membrane-forming phospholipids. Consequently, phospholipid membranes mixed with PEG-lipid at more than 5-10% mole fraction tend to generate highly curved micelles. Despite this membrane-disruptive tendency of PEG-lipid at high concentrations, low concentrations appear both compatible with vesicle morphology and technologically useful. Upon injection into the circulation, these so-called 'stealthy' PEG-liposomes are cleared more slowly ( $\tau_{1/2} \sim 10-15$  hr) than conventional liposomes ( $< 1$  hr) from the blood by phagocytes within the liver and spleen [69,70]. As a result of their extended circulation time, stealth vesicles loaded with anticancer drugs such as doxorubicin circulate

sufficiently long to find their way into well-hidden but relatively high permeability tumors [71] – as also described below for controlled release polymersomes.

PEGylation is clearly useful for biomedical application and has raised the question as to whether a polymersome-type system composed 100% of PEG-polymer would work as well in vivo. There were reasons to anticipate significant improvements, especially since stable anchorage in liposomes of large hydrophilic PEG chains seems limited: incubations in serum had shown that liposomes immediately lose approximately one-third of their PEG-lipids, presumably owing to facilitated micellization [72]. In contrast, polymersome architectures are founded on more proportional and larger amphiphilic polymers, leading to more stable anchorage and no measurable decrease in vesicle size or loss of copolymer in serum [28]. Moreover, the far greater hydrophilic PEG (100%) content should confer better resistance to plasma protein deposition (known as ‘opsonization’) and thereby extend vesicle circulation times. The dense and stable PEG brush does delay opsonization, but selective protein deposition eventually occurs after 10-20 hr. This was determined by quickly and carefully collecting polymersomes after incubation in plasma and analysing the vesicle-bound protein by gel electrophoresis (Fig. 3A) [29]. The molecular weight of the detected protein (~40-45 kD) suggests deposition of a fragment of the plasma protein C3 or else perhaps fibronectin, both of which could mediate adhesion to cells. Indeed, the deposition of plasma protein is sufficient to convert polymersomes from vesicles that are initially invisible to phagocytic cells to highly adhesive vesicles that bind to such cells and are then internalized (Fig. 3B).

Injection of polymersomes into the blood circulation of rats and mice shows prolonged circulation [29]. Clearance half-lives range from 15-30 h and significantly exceed the circulation times of stealth liposomes in similar dose injections. When half-life data for liposomes and polymersomes with ~2000 Da PEG chains is compared by plotting  $\tau_{1/2}$  as a function of %-PEGylation, an excellent fit is provided by a Langmuir type binding isotherm. This suggests that a critical level of membrane surface opsonization,  $c^* \sim 1/\tau_{1/2}$ , is required and that PEG delays protein deposition in a systematic fashion. Indeed, fits of  $\tau_{1/2}$  versus  $M_{\text{PEG}}$  suggest a scaling (with exponent  $a = 0.43$ ) that is similar to the scaling with  $M$  of both core thickness  $d$  (exponent  $b = 0.55$ ) and brush thickness  $d_{\text{brush}}$ . Such efforts *with liposomes* to determine the  $M_{\text{PEG}}$  dependence of  $\tau_{1/2}$  were frustrated in the past by the tendency of higher molecular weight PEG chains to micellize because PEG-lipids have high  $f$ . The recent results with polymersomes thus establish perhaps for the first time that a brushy layer is a kinetic barrier to deposition of opsonizing proteins and that the barrier effectiveness depends simply on brush thickness.

## 5. POLYMERSOME LOADING AND DELIVERY

Progress in loading polymersomes with compounds that should be active in vivo has generally kept pace with the developments above. Seeing is believing and a good starting point for loading, and so a combination of analytical methods and imaging of micron-sized ‘giant’ vesicles with fluorescent or light-absorbing compounds have been used to show that polymersomes will encapsulate various hydrophilic drugs, proteins, and nucleic acids. The water-soluble, anti-cancer drug doxorubicin mentioned before has a red fluorescence and is efficiently encapsulated within polymersomes post-formation by pH-gradient methods established for liposomes [51,73]. Proteins are also, of course, being encapsulated within polymer vesicles, and extension of early work on polymersome-encapsulated hemoglobin [28] now demonstrates oxygen affinities similar to that of human red blood cells [74]. As cited above, DNA has been virally injected into polymersomes in a ‘nano tour de force’ that exploits pre-integrated channel proteins [65]. Less elegant but adequate means of

encapsulation are presently being applied by us to anti-sense molecules (~10-20 nucleotides) with some initial success in gene therapy in vivo (Y. Kim et al, unpublished).

Many fluorescent dyes and drugs have been integrated into the hyperthick hydrophobic cores of polymersome membranes. Perhaps among the most useful for its translational potential is the insoluble, clinically used anti-cancer drug Taxol that, in fluorescent form, makes giant vesicles visible with a rim-bright fluorescence. This drug intercalates at molar ratios that exceed those of liposomes as confirmed by analytical gel filtration following dialysis [51]. Biocompatible fluorescent dyes have been routinely used at low concentrations to track the fate of polymersomes both in cell culture and in vivo [29]. Infrared fluorescence dyes that might be useful for deep tissue imaging [75] are also being integrated into the membranes of polymersomes in the hopes of imaging tumors. Lastly, the environmentally-sensitive amphiphilic dye LAURDAN has also been integrated and used to probe binding of surface-active peptides [68].

While the above list of integrated or encapsulated compounds is hardly exhaustive and is rapidly growing, functional tests of loaded and degradable, long-circulating polymersomes are also emerging. There are many mouse models of human disease that span the range from mice with tumors to genetically engineered mice with mutations in one or more proteins. Successful therapy of these diseased animals might eventually translate to humans – one would hope – and might also require the sort of cell-directed targeting that some viruses exploit. On the other hand, most liposomes and many other carriers that have been successfully translated into clinical use over the years exploit “passive targeting” for tissue localization through permeation of a leaky vasculature. This appears common in diseased and damaged tissue and can also involve, perhaps, non-specific mechanisms of cellular uptake such as fluid-phase endocytosis (pinocytosis). These processes are the essence of the enhanced permeation and *retention* (EPR) effect described first perhaps for rapidly growing solid tumors [76]. Thus, in the EPR effect, passively targeted carriers – if small enough – will localize at the intended site, enter cells perhaps, and release drug instead of rapidly flowing in the blood past the site.

### 5.1 Shrinking tumors with polymersomes

Polymersomes loaded with two anti-cancer drugs, taxol (TAX) in the hyperthick membrane and doxorubicin (DOX) in the lumen (Fig. 4A), constitute a potent cocktail to direct drugs to two distinct cellular targets, namely microtubules for TAX and DNA for DOX. Drug resistance of individual tumor cells treated with both drugs at the same time would seem likely to be minimized by such a strategy. Combining this idea with both the long circulation capability to sustainably exploit the EPR effect of tumors and also the controlled release mechanisms that are accelerated in the low pH within cellular endolysosomes (and also tumors perhaps) seemed sufficiently interesting to begin animal studies of tumor shrinkage with drug-loaded polymersomes. DOX and TAX are also two of the most common anticancer drugs used in the clinic and so the barriers along the translational path appear smaller than with new drugs.

Before attempting treatment of any tumor-bearing mice, one needs to first assess the Maximum Tolerated Dose (MTD) of carrier and drug combinations that mice can tolerate (in mg drug / kg body weight). This is most simply established by examining weight loss and defining the MTD by loss of 5% of initial body weight 24 hr after injection [55,56]. Such studies and many additional characterizations (including multiple injections over many weeks) show that various polymersome formulations of interest for drug delivery cause no detectable weight loss. Additionally, the MTD of drugs in polymersomes also proves several-fold higher than that of free drugs, which is consistent with sustained drug sequestration within the circulating vesicles.

Cancer continues to be one of the leading causes of death for young and old, and the challenges of translating cancer therapy results from model systems to humans are many. Nonetheless, one standard starting point is to implant human-derived cancer cells in ‘nude’ mice. These mice have an impaired immune system and do not reject the foreign cells. This animal model system proves remarkably reproducible, with a large fraction of mice exhibiting tumors of very similar size ( $\sim\text{cm}^2$  in area per Fig. 4B). In a typical study, four mice or more per treatment group are given one intravenous injection of either free drug, polymersome-drug, saline, or empty polymersomes. Measurements of tumor size over the subsequent week post-injection are completed by sacrificing the mice and isolating the tumors for examination of both DOX localization and direct biochemical assay of cell death.

Injection of saline and empty polymersomes show no difference and do not slow the rapid growth of the tumor, which is almost 3-fold larger after 5 days (Fig. 4C - inset) [55,56]. Injection of the free drug DOX + TAX cocktail briefly delays tumor growth, but does not shrink the tumor. However, a single intravenous injection of PEG-PLA polymersomes loaded with DOX + TAX sustainably shrinks the tumor (Fig. 4C).

Isolation of tumors at 24 hr followed by slicing thin-sections of the tumors for microscopic imaging of DOX fluorescence shows diffuse red fluorescence for free drugs and punctate red fluorescence for polymersome delivered drugs (Fig. 4D). The tumor intensity of DOX injected as free drug is considerably less than with polymersome delivery, and the amount of ‘free drug DOX’ in the tumor peaks within hours rather than near one day for DOX-polymersomes [55].

Combination therapy with (DOX + TAX)-loaded polymersomes triggers massive cell death or cell suicide known as ‘apoptosis’ in the tumors. Within 1 day of treatment, fluorescence staining for cell death is strongly positive (Fig. 4D). Based on more quantitative methods, apoptosis is enhanced 2-fold with polymersome-delivered drug *versus* free drug, and a >25-fold increase is seen relative to both untreated and empty vesicle treatments. Consistent with tumor re-growth after injection of free drug, apoptosis with free drugs decreases with time. In contrast, high levels of apoptosis appear more sustained for polymersome-based delivery. This first polymersome-based therapeutic may be just the first of many more to come.

## 6. POLYMERSOMES OF MORE COMPLEX DESIGN

The surface of a virus is more complex in composition than the polymersomes described above. Many if not most mammalian viruses are enveloped by a cell-derived lipid bilayer. The membrane coats the capsid during viral export from the host cell in which viral multiplication occurs. Viral envelope proteins and capsid-associated proteins protrude through the lipid bilayer and might contribute targeting roles to viruses, while the underlying capsid confers robustness to the composite structure. Although the enveloping process tends to yield a more host-compatible structure, the viruses present many targets or epitopes (proteins, lipids, and nucleic acid) for the immune system to mount a response to. Indeed, “successful” viruses such as influenza and HIV constantly evolve their proteins and evade the host immune system, whereas less successful viruses today (eg. – the polio virus) do not evolve so readily and are (thankfully) immunized against. Another aspect of this immunogenicity is that viruses being developed for gene therapy generally prompt an immune response, which means that they might only be used once before the body's immune system becomes a barrier to any follow-up therapy. The important point is that viruses have been around for eons and immune systems have evolved to successfully deal with most viruses. In contrast, synthetic polymers have been around for no more than a century and appear to have little to no immunogenicity. Although the results for polymersomes reviewed above show that any immune privilege of these fully PEGylated systems do not extend

indefinitely to processes such as protein deposition (opsonization) and phagocytosis, the simple polymersome platforms outlined above might be re-engineered for improved performance.

A neutral brush of PEG usefully extends circulation times, but cell membranes are negatively charged and so some negative charge in the brush might usefully inhibit non-specific uptake by cells. In addition, targeting mechanisms might be added to the brush with peptides or other moieties, but the controlled release mechanisms based on polyester hydrolysis or other polymer reactions might also be made more site specific with short peptides that can be cleaved by specific proteases. These are just a few of the many possibilities that motivate new chemistries. One should always keep in mind, however, that in biomedical applications new chemistries bring new possibilities of toxicity and immunogenicity, and so simplicity should always temper complex chemical designs.

### 6.1 Charged Polymersomes and Peptide-Based Vesicles

Although charged liposomes tend to be cleared quickly from the circulation [37,77], the addition of charge to polymer amphiphiles presents further opportunities for controlled release in response to external stimuli, such as pH (e.g., PAA-mediated endolysosomal rupture [78]). However, the shape and structure of charged diblock copolymer aggregates in solution are governed by an especially delicate balance of forces. Interfacial tension between the core and the bulk solvent continues to orient, confine, and stretch the chains, but the interactions between solvated corona blocks can be repulsive, through sterics and electrostatics, as well as attractive, if multivalent ions are involved [3]. Eisenberg and coworkers [79] mapped out the first morphological phase diagram of charged diblock copolymers in dilute solution for “crew-cut” PAA-PS copolymers. The rich phase behavior and dynamics of a relatively symmetric PAA-PBD diblock have now also been mapped out in water [80]. Depending on the concentration of added calcium or sodium salt as well as pH, these diblocks are seen to self-assemble in water into stable vesicles, worms, and spheres. Furthermore, using fluorescence microscopy, researchers visualized transitions of vesicles into worms and spheres within minutes with a sudden increase of pH or chelation of salt. Liu & Eisenberg [81] have likewise shown rapid pH-triggered inversion of amphiphilic triblock copolymer vesicles of PAA-PS-poly(4-vinyl pyridine) in organic/aqueous mixtures. With increasing bulk pH, the aggregate morphology changes from vesicles, with poly(4-vinyl pyridine) outside, to solid aggregates and then inverts back into a whole vesicle assembly, with PAA on the outside. Some of these design principles seem likely to make their way into biocompatible polymersomes and certainly inform us about the dramatic effects of charge in polymer systems.

A rapidly emerging approach to polymer-based vesicles involves a return to biology with peptide-based assemblies. In contrast to viral capsids with lock-and-key assemblies of great precision, the peptide-based vesicle assemblies have amphiphilicity as their foundation. Emerging results from several groups suggest there is no need for nature's lock-and-key approach, in principle. For example, PBD-(poly-*L*-glutamic acid) diblock copolymers self-assemble in aqueous solution into vesicles (peptosomes) [82] in which the hydrophilic polypeptide segment forms a well-defined secondary structure of  $\alpha$ -helix. In dilute aqueous solutions, the copolymers form either spherical micelles or larger vesicular aggregates. In addition, these systems exhibit pH- and ionic-strength-dependent changes in hydrodynamic radius and in coil-helix transitions. In addition to providing the hydrophobic driving forces for self-assembly, the PBD block can be laterally cross-linked [50,83]; this and related cross-linking [63] covalently capture the aggregate in a shape-persistent nanoparticle [84]. Such nanoparticles may be suitable for applications such as encapsulation or release of hydrophilic and hydrophobic active species or in sensor nanodevices, where the latter

systems could take advantage of protein channels that – perhaps surprisingly – will integrate into the hyperthick block copolymer membranes [19,64].

Hybrid block copolymers constructed from amphiphilic  $\beta$ -strand peptide sequences and PEG have recently been studied [85]. In comparison with the native peptide sequence, di- and triblock copolymers with PEG were shown to stabilize the peptide's secondary structure against pH variation and to self-assemble into helical tapes that stack into fibrils. Vesicles have not been reported but seem feasible by this approach. Conversely, diblock copolypeptides of {poly( $N_{\epsilon}$ -2-(2-(2-methoxyethoxy)ethoxy)acetyl-*L*-lysine)-(poly-*L*-leucine)} have been shown to self-assemble into bilayer vesicles whose size and structure are dictated primarily by the ordered conformations of the peptide segments [86], in a manner similar to viral capsid assembly. If 70% of the *L*-leucine in the hydrophobic domain is replaced in a statistical manner with *L*-lysine, the system becomes pH sensitive. At pH 9, vesicles form, but protonation of the lysine residues enhances their hydrophilicity and destabilizes the  $\alpha$ -helical structure of the leucine-rich domain owing to electrostatic repulsion of the like charges. These helix-to-coil transitions destabilize the vesicular assembly, leading to porous membranes or complete disassociation of the structures. Recent extensions of polymer-peptide hybrids include the attachment of hydrophobic polymers such as PS to enzymes with the subsequent self-assembly into spherical aggregates and vesicles that still retain biological activity [87,88].

## 6.2 Active Targeting of Polymersomes

Although few if any drug carriers in clinical use today are targeted, viruses often show preferential – though not exclusive – interactions with particular cell types and cell entry pathways. Given that polymersomes exhibit minimal nonspecific adhesion to cells (initially), that they can circulate for many tens of hours, and that they can integrate controlled release mechanisms, targeted polymersomes should add an additional level of viral mimicry. With PEG-based assemblies, much work has been focused on attaching ligands or antibodies to the hydroxyl end-group [89,90]. Biotinylation of nondegradable PEG-PBD diblocks [91] has allowed block copolymer assemblies to attach to (a) surfaces coated with the biotin receptor avidin as well as to (b) cells where the assemblies successfully delivered the hydrophobic cytotoxic drug Taxol<sup>®</sup>. Similar chemistry has been used to attach either an antihuman IgG or antihuman serum to PEG-carbonate- or PEG-polyester-assembled polymer vesicles [52,92]. Meier and coworkers [93] have modified their triblock copolymer polymersomes with polyguanylic acid to target a macrophage scavenger receptor SRA1. This scavenger receptor is a pattern-recognition antigen upregulated only in activated tissue macrophages, not in monocytes or monocyte precursor cells. Though promising, these in vitro cell targeting studies have not been translated to in vivo conditions, where opsonization by serum components and competitive interactions with other cells often impede and complicate targeting efforts [90]. Moreover, targeting via attached chemical groups – even if it were to provide a major advantage and justify the added complexity from a regulatory standpoint – does not act like a ‘magnet’ with action at a distance; convective and/or diffusive collisions of the carrier with a cell must occur for targeted adhesion to take place. Retention of a multi-valent adhesion of the carrier on the cell surface can then foster uptake or localized release, but if a carrier localizes within a tissue or tumor where convective and/or diffusive forces are minimal, then such retention offers little additional advantage. This is the essence of passive targeting by the enhanced permeation and *retention* (EPR) effect [76].



## 7. CONCLUSIONS

Polymersomes broaden considerably the choice of vesicle chemistries, molecular weights, and self-assembled structures for application. Comparisons to viruses are perhaps more insightful since high stability of polymersomes means that controlled release mechanisms, cell entry, bio-distribution, and other features such can be separately engineered in. Initial successes in cancer treatment as well as a broad spectrum of functionality suggests these synthetic carrier systems offer a generic approach for drug delivery.

## Acknowledgments

Collaborations with Prof. F.S. Bates during the early stages of our work on polymer vesicles are very gratefully acknowledged. Support for work from the Discher group, reviewed in broader context here, has been provided by grants from the NIH, NSF-PECASE, and Penn's NanoTechnology Institute and NSF-MRSEC.

## REFERENCES

1. Discher DE, Ahmed F. Polymersomes. *Annu Rev Biomed Eng.* 2006; 8:323–41. [PubMed: 16834559]
2. Michel JP, Ivanovska IL, Gibbons MM, Klug WS, Knobler CM, Wuite GJ, Schmidt CF. Nanoindentation studies of full and empty viral capsids and the effects of capsid protein mutations on elasticity and strength. *Proc Natl Acad Sci U S A.* Apr 18; 2006 103(16):6184–9. [PubMed: 16606825]
3. Israelachvili, JN. *Intermolecular and Surface Forces.* Academic Press Ltd.; San Diego: 1991.
4. Luo LB, Eisenberg AJ. Thermodynamic stabilization mechanism of block copolymer vesicles. *J. Am. Chem. Soc.* 2001; 123:1012–13. [PubMed: 11456651]
5. Ortiz V, Nielsen S, Klein ML, Discher DE. Computer simulation of aqueous diblock copolymer assemblies – length scales and methods. *Journal of Polymer Science B – Polymer Physics.* 2006; 44:1907–1918.
6. MacKerell AD, Bashford D, Bellott M, Dunbrack RL, Evanseck JD, Field MJ, Fischer S, Gao J, Guo H, Ha S, Joseph-McCarthy D, Kuchnir L, Kuczera K, Lau FTK, Mattos C, Michnick S, Ngo T, Nguyen DT, Prodhom B, Reiher WE, Roux B, Schlenkrich M, Smith JC, Stote R, Straub J, Watanabe M, Wiorkiewicz-Kuczera J, Yin D, Karplus M. All-atom empirical potential for molecular modeling and dynamics studies of proteins. *J. Phys. Chem. B.* 1998; 102:3586–3616.
7. Pearlman DA, Case DA, Caldwell JW, Ross WS, Cheatham TE, Debolt S, Ferguson D, Seibel G, Kollman P. AMBER, a package of computer-programs for applying molecular mechanics, normal-mode analysis, molecular dynamics, and free energy calculations to simulate the structural and energetic properties of molecules. *Comput. Phys. Commun.* 1995; 91:1–41.
8. Jorgensen WL, Maxwell DS, Tirado-Rives J. Development and testing of the OPLS all-atom force field on conformational energetics and properties of organic liquids. *J. Am. Chem. Soc.* 1996; 118:11225–36.
9. Anderson PM, Wilson MR. Molecular dynamics simulations of amphiphilic graft copolymer molecules at a water/air interface. *J. Chem. Phys.* 2004; 121:8503–10. [PubMed: 15511174]
10. Miller AF, Wilson MR, Cook MJ, Richards RW. Monte Carlo simulations of an amphiphilic polymer at a hydrophobic/hydrophilic interface. *Mol. Phys.* 2003; 101:1131–38.
11. Khalatur PG, Khokhlov AR, Nyrkova IA, Semenov AN. Aggregation processes in self-associating polymer systems: Computer simulation study of micelles in the superstrong segregation regime. *Macromol. Theory Simul.* 1996; 5:713–747.
12. Goetz R, Gompper G, Lipowsky R. Mobility and elasticity of self-assembled membranes. *Phys. Rev. Lett.* 1999; 82:221–4.
13. Termonia Y. Sphere-to-cylinder transition in dilute solutions of diblock copolymers. *J. Polym. Sci. Pt. B-Polym. Phys.* 2002; 40:890–5.
14. Yamamoto S, Maruyama Y, Hyodo S. Dissipative particle dynamics study of spontaneous vesicle formation of amphiphilic molecules. *J. Chem. Phys.* 2002; 116:5842–49.

15. Maiti PK, Lansac Y, Glaser MA, Clark NA, Rouault Y. Self-assembly in surfactant oligomers : A course-grained description through molecular dynamics simulations. *Langmuir*. 2002; 18:1908–18.
16. Srinivas G, Shelley JC, Nielsen SO, Discher DE, Klein ML. Simulation of diblock copolymer self-assembly, using coarse-grain model. *J. Phys. Chem. B*. 2004; 108:8153–60.
17. Srinivas G, Discher DE, Klein ML. Self-assembly and properties of diblock copolymers by coarse-grain molecular dynamics. *Nat. Mater*. 2004; 3:638–44. [PubMed: 15300242]
18. Srinivas G, Klein ML. Coarse-grain molecular dynamics simulations of diblock copolymer surfactants interacting with a lipid bilayer. *Mol. Phys*. 2004; 102:883–9.
19. Srinivas G, Discher DE, Klein ML. Key roles for chain flexibility in block copolymer membranes that contain pores or make tubes. *Nano Letters*. 2005; 5:2343–49. [PubMed: 16351175]
20. Bermudez H, Brannan AK, Hammer DA, Bates FS, Discher DE. Molecular weight dependence of polymersome membrane structure, elasticity, and stability. *Macromolecules*. 2002; 35:8203–8.
21. Warren PB. Dissipative particle dynamics. *Curr. Opin. Colloid Interface Sci*. 1998; 3:620–4.
22. Peters EAJF. Elimination of time step in DPD. *Europhys. Lett*. 2004; 66:311–7.
23. Trofimov SY, Nies ELF, Michels MAJ. Constant-pressure simulations with dissipative particle dynamics. *J. Chem. Phys*. 2005:123.
24. Yamamoto S, Hyodo S. Budding and fission dynamics of two-component vesicles. *J. Chem. Phys*. 2003; 118:7937–43.
25. Ortiz V, Nielsen SO, Discher DE, Klein ML, Lipowsky R, Shillcock J. Dissipative particle dynamics of simulations of polymersomes. *J. Phys. Chem. B*. 2005; 109:17708–14. [PubMed: 16853266]
26. Discher BM, Won YY, Ege DS, Lee JCM, Bates FS, Discher DE, Hammer DA. Polymersomes: Tough vesicles made from diblock copolymers. *Science*. 1999; 284:1143–46. [PubMed: 10325219]
27. Lee JCM, Santore M, Bates FS, Discher DE. From membrane to melts, rouse to reptation: diffusion in polymersome versus lipid bilayers. *Macromolecules*. 2002; 35:323–26.
28. Lee JCM, Bermudez H, Discher BM, Sheehan MA, Won YY, Bates FS, Discher DE. Preparation, stability, and in vitro performance of vesicles made with diblock copolymers. *Biotechnol. Bioeng*. 2001; 73:135–45. [PubMed: 11255161]
29. Photos PJ, Bacakova L, Discher BM, Bates FS, Discher DE. Polymer vesicles in vivo: correlations with PEG molecular weight. *J. Control. Release*. 2003; 90:323–34. [PubMed: 12880699]
30. Discher DE, Eisenberg A. Polymer vesicles. *Science*. 2002; 297:967–73. [PubMed: 12169723]
31. Hamley IW. Nanoshells and nanotubes from block copolymers. *Soft Matter*. 2005; 1:36–43.
32. Battaglia G, Ryan AJ. Polymeric vesicle permeability: a facile chemical assay. *Langmuir*. 2006; 22:4910–3. [PubMed: 16700572]
33. Dimova R, Seifert U, Pouligny B, Forster S, Dobereiner HG. Hyperviscous diblock copolymer vesicles. *Euro. Phys. J E*. 2002; 7:241–50.
34. Aranda-Espinoza H, Bermudez H, Bates FS, Discher DE. Electromechanical limits of polymersomes. *Phys. Rev. Lett*. 2001; 87:208301. [PubMed: 11690515]
35. Battaglia G, Ryan AJ. Bilayers and interdigitation in block copolymer vesicles. *J Am. Chem. Soc.* Jun 22; 2005 127(24):8757–64. [PubMed: 15954782]
36. Lasic, DD.; Papahadjopoulos, D. *Medical Applications of Liposomes*. Elsevier Science; Amsterdam: 1998.
37. Semple SC, Chonn A, Cullis PR. Interactions of liposomes and lipid-based carrier systems with blood proteins: relation to clearance behaviour in vivo. *Adv. Drug Deliv. Rev*. 1998; 32:3–18. [PubMed: 10837632]
38. Karathanasis E, Ayyagari AL, Bhavane R, Bellamkonda RV, Annapragada AV. Preparation of in vivo cleavable agglomerated liposomes suitable for modulated pulmonary drug delivery. *J. Cont. Release*. 2005; 103:159–75.
39. Jorgensen K, Davidsen J, Mouritsen OG. Biophysical mechanisms of phospholipase A2 activation and their use in liposome-based drug delivery. *FEBS Lett*. 2002; 531:23–27. [PubMed: 12401197]

40. Shin J, Shum P, Thompson DH. Acid-triggered release via depegylation of dope liposomes containing acid-labile vinyl ether peg-lipids. *J. Cont. Release.* 2003; 91:187–200.
41. Jain S, Bates FS. On the origins of morphological complexity in block copolymer surfactants. *Science.* 2003; 300:460–64. [PubMed: 12702869]
42. Gref R, Minamitae Y, Peracchia MT, Trubetskoy V, Torchillin V, Langer R. Biodegradable long-circulating polymeric nanospheres. *Science.* 1994; 263:1600–3. [PubMed: 8128245]
43. Yasugi K, Nagasaki Y, Kato M, Kataoka K. Preparation and characterization of polymer micelles from poly(ethylene glycol)-poly(D,L-lactide) block copolymers as potential drug carrier. *J. Control. Release.* 1999; 62:89–100. [PubMed: 10518640]
44. Batycky RP, Hanes J, Langer R, Edwards DA. A theoretical model of erosion and macromolecular drug release from biodegrading microspheres. *J. Pharm. Sci.* 1997; 86:1464–77. [PubMed: 9423163]
45. Hagan SA, Coombes AGA, Garnett MC, Dunn SE, Davies MC, et al. Polylactide-poly(ethylene glycol) copolymers as drug delivery systems. I. Characterization of water dispersible micelle-forming systems. *Langmuir.* 1996; 12:2153–61.
46. Kim Y, Dalhaimer P, Christian DA, Discher DE. Polymeric worm micelles as nano-carriers for drug delivery. *Nanotechnology.* 2005; 16:S484–91. [PubMed: 21727469]
47. Geng Y, Discher DE. Hydrolytic degradation of poly(ethylene oxide)-block-polycaprolactone worm micelles. *J. Am. Chem. Soc.* 2005; 127:12780–81. [PubMed: 16159254]
48. Kim HK, Park TG. Surface stabilization of diblock PEG-PLGA micelles by polymerization of N-vinyl-2-pyrrolodone. *Macromol. Rapid Commun.* 2002; 23:26–31.
49. Savic R, Luo L, Eisenberg A, Maysinger D. Micellar nanocontainers distribute to defined cytoplasmic organelles. *Science.* 2003; 300:615–18. [PubMed: 12714738]
50. Ahmed F, Hategan A, Discher DE, Discher BM. Block copolymer assemblies with cross-link stabilization: from single-component monolayers to bilayer blends with PEO-PLA. *Langmuir.* 2003; 19:6505–11.
51. Ahmed F, Discher DE. Self-porating polymersomes of PEG-PLA and PEGPCL: hydrolysis-triggered controlled release vesicles. *J. Control. Release.* 2004; 96:37–53. [PubMed: 15063028]
52. Meng F, Engbers GHM, Feijen J. Biodegradable polymersomes as a basis for artificial cells: encapsulation, release and targeting. *J. Conl. Release.* 2005; 101:187–98.
53. Lee Y, Chang JB, Kim HK, et al. Stability studies of biodegradable polymersomes prepared by emulsion solvent evaporation method *Macromol. Res.* Jun; 2006 14(3):359–364.
54. Ghoroghchian PP, Li GZ, Levine DH, et al. Bioresorbable vesicles formed through spontaneous self-assembly of amphiphilic poly(ethylene oxide)-block-polycaprolactone. *Macromol. Mar 7; 2006 39(5):1673–1675.*
55. Ahmed F, Pakunlu RI, Brannan A, Bates F, Minko T, Discher DE. Biodegradable polymersomes loaded with both paclitaxel and doxorubicin permeate and shrink tumors, inducing apoptosis in proportion to accumulated drug. *J Cont. Release.* 2006 Epub ahead of print.
56. Ahmed F, Pakunlu RI, Srinivas G, Brannan A, Bates FS, Klein ML, Minko T, Discher DE. Shrinkage of a Rapidly Growing Tumor by Drug-loaded Polymersomes: pH-Triggered Release through Copolymer Degradation. *Mol. Pharm.* 2006; 3:340–50. 2006. [PubMed: 16749866]
57. Napoli A, Boerakker MJ, Tirelli N, Nolte RJM, Sommerdijk NAJM, Hubbell JA. Glucose-oxidase based self-destructing polymeric vesicles. *Langmuir.* 2004; 20:3487–91. [PubMed: 15875368]
58. Borchert U, Lipprandt U, Bilanz M, et al. pH-induced release from P2VP-PEO block copolymer vesicles. *Langmuir.* JUN 20. 2006; 22(13):5843–5847. [PubMed: 16768517]
59. Ruyschaert T, Sonnen AFP, Haefele T, Meier W, Winterhalter M, Fournier D. Hybrid nanocapsules: interactions of ABA block copolymers with liposomes. *J. Am. Chem. Soc.* 2005; 127:6242–47. [PubMed: 15853329]
60. Sonawane ND, Szoka FC, Verkman AS. Chloride accumulation and swelling in endosomes DNA transfer by polyamine-DNA polyplexes. *J. Biol. Chem.* 2003; 278:44826–31. [PubMed: 12944394]
61. Barron LG, Gagne L, Szoka FC. Lipoplex-mediated gene delivery to the lung occurs within 60 minutes of intravenous administration. *Hum. Gene Ther.* 1999; 10:1683–94. [PubMed: 10428213]

62. Moghimi SM, Hunter AC, Murray JC, Szweczyk A. Cellular distribution of nonionic micelles. *Science*. 2004; 303:626–27. [PubMed: 14752144]
63. Nardin C, Hirt T, Leukel J, Meier W. Polymerized ABA triblock copolymer vesicles. *Langmuir*. 2000; 16:1035–41.
64. Meier W, Nardin C, Winterhalter M. Reconstitution of channel proteins in (polymerized) ABA triblock copolymer membranes. *Angew. Chem. Int. Ed. Engl.* 2000; 39:4599–602. [PubMed: 11169683]
65. Graff A, Sauer M, Van Gelder P, Meier W. Virus-assisted loading of polymer nanocontainer. *Proc. Nat. Acad. Sci. of U.S.A.* 2002; 99:5064–8.
66. Wong D, Jeon TJ, Schmidt J. Single molecule measurements of channel proteins incorporated into biomimetic polymer membranes. *Nanotechnology*. Aug 14; 2006 17(15):3710–3717.
67. Ho D, Chu B, Lee H, Montemagno CD. Protein-driven energy transduction across polymeric biomembranes. *Nanotechnology*. Aug; 2004 15(8):1084–1094.
68. Vijayan K, Discher DE, Lal J, Janmey P, Goulian M. Interactions of membrane-active peptides with thick, neutral, nonzwitterionic bilayers. *J. Phys. Chem. B*. Aug 4; 2005 109(30):14356–14364. [PubMed: 16852806]
69. Woodle MC. Surface-modified liposomes---assessment and characterization for increased stability and prolonged blood circulation. *Chem. Phys. Lipids*. 1993; 64:249–62. [PubMed: 8242837]
70. Klivanov AL, Maruyama K, Torchilin VP, Huang L. Amphipathic polyethyleneglycols effectively prolong the circulation times of liposomes. *FEBS Lett.* 1990; 268:235–37. [PubMed: 2384160]
71. Hong R-L, Huang C-J, Tseng Y-L, Pang VF, Chen S-T, Liu J-J, Chang F-H. *Clinical Cancer Research*. 1999; 5:3645–3652. [PubMed: 10589782]
72. Bradley AJ, Devine DV, Ansell SM. Inhibition of liposome-induced complement activation by incorporated poly(ethylene glycol) lipids. *Arch. Biochem. Biophys.* 1998; 357:185–94. [PubMed: 9735159]
73. Choucair A, Soo PL, Eisenberg A Active loading and tunable release of doxorubicin from block copolymer vesicles. *Langmuir*. Sep 27; 2005 21(20):9308–9313. [PubMed: 16171366]
74. Arifin DR, Palmer AF. Polymersome encapsulated hemoglobin: a novel type of oxygen carrier. *Biomacromolecules*. 2005; 6:2172–81. [PubMed: 16004460]
75. Lin VS, DiMagno SG, Therien MJ. Highly conjugated, acetylenyl bridged porphyrins: new models for light-harvesting antenna systems. *Science*. May 20; 1994 264(5162):1105–11. [PubMed: 8178169]
76. Maeda, H. Enhanced permeability and retention (EPR) effect: basis for drug targeting to tumor.. In: Muzykantov, VR.; Torchilin, VP., editors. *Biomedical Aspects of Drug Targeting*. Kluwer Academic; Boston: 2002. p. 211–278.
77. Liu DX, Liu F, Song YK. Recognition and clearance of liposomes containing phosphatidylserine are mediated by serum opsonin. *Biochim. Biophys. Acta*. 1995; 1235:140–46. [PubMed: 7718601]
78. Jones RA, Cheung CY, Black FE, Zia JK, Stayton PS, et al. Poly(2-alkylacrylic acid) polymers deliver molecules to the cytosol by pH-sensitive disruption of endosomal vesicles. *Biochem. J.* 2003; 372:65–75.
79. Zhang L, Yu K, Eisenberg A. Ion-induced morphological changes in “crewcut” aggregates of amphiphilic block copolymers. *Science*. 1996; 272:1777–79. [PubMed: 8662482]
80. Geng Y, Ahmed F, Bhasin N, Discher DE. Visualizing worm micelle dynamics and phase transitions of a charged diblock copolymer in water. *J. Phys. Chem. B*. 2005; 109:3772–79. [PubMed: 16851424]
81. Liu F, Eisenberg A. Preparation and pH triggered inversion of vesicles from poly(acrylic acid)-block-polystyrene-block-poly(4-vinyl pyridine). *J. Am. Chem. Soc.* 2003; 125:15059–64. [PubMed: 14653740]
82. Kukula H, Schlaad H, Antonietti M, Forster S. The formation of polymer vesicles or “peptosomes” by polybutadiene-block-poly(l-glutamate)s in dilute aqueous solution. *J. Am. Chem. Soc.* 2002; 124:1658–63. [PubMed: 11853440]
83. Discher BM, Bermudez H, Hammer DA, Discher DE, Won Y-Y, Bates FS. Cross-linked polymersome membranes: vesicles with broadly adjustable properties. *J. Phys. Chem. B*. 2002; 106:2848–54.

84. Checot F, Lecommandoux S, Klok H-A, Gnanou Y. From supramolecular polymersomes to stimuli-responsive nano-capsules based on poly(diene-b-peptide) diblock copolymers. *Eur. Phys. J. E Soft Matter*. 2003; 10:25–35. [PubMed: 15011076]
85. Hamley IW, Ansari IA, Castelletto V, Nuhn H, Rosler A, Klok H-A. Solution self-assembly of hybrid block copolymers containing poly(ethylene glycol) and amphiphilic  $\beta$ -strand peptide sequences. *Biomacromolecules*. 2005; 6:1310–15. [PubMed: 15877346]
86. Bellomo EG, Wyrsta MD, Pakstis L, Pochan DJ, Deming TJ. Stimuli-responsive polypeptide vesicles by conformation-specific assembly. *Nat. Mater*. 2004; 3:244–48. [PubMed: 15034560]
87. Boerakker MJ, Hannink JM, Bomans PHH, Frederik PM, Nolte RJM, et al. Giant amphiphiles by cofactor reconstitution. *Angew. Chem. Int. Ed. Engl*. 2002; 41:4239–41. [PubMed: 12434350]
88. Velonia K, Rowan AE, Nolte RJM. Lipase polystyrene giant amphiphiles. *J. Am. Chem. Soc*. 2002; 124:4224–25. [PubMed: 11960447]
89. Torchilin VP, Levchenko TS, Lukyanov AN, Khaw BA, Klivanov AL, et al. p-nitrophenylcarbonyl-PEG-PE-liposomes: fast and simple attachment of specific ligands, including monoclonal antibodies, to distal ends of PEG chains via p-nitrophenylcarbonyl groups. *Biochim. Biophys. Acta*. 2001; 1511:397–411. [PubMed: 11286983]
90. Discher, DE.; Photos, P.J.; Ahmed, F.; Parthasarathy, R.; Bates, FS. Polymersomes: a new platform for drug targeting.. In: Muzykantov, VR.; Torchilin, VP., editors. *Biomedical Aspects of Drug Targeting*. Kluwer Academic; Boston: 2002. p. 459-471.
91. Dalhaimer P, Engler A, Parthasarathy R, Discher DE. Targeted worm micelles. *Biomacromolecules*. 2004; 5:1714–19. [PubMed: 15360279]
92. Lin JJ, Ghoroghchian PP, Zhang Y, Hammer DA. Adhesion of antibody-functionalized polymersomes. *Langmuir*. Apr 25; 2006 22(9):3975–9. [PubMed: 16618135]
93. Broz P, Benito SM, Saw CL, Burger P, Heider H, et al. Cell targeting by a generic receptor-targeted polymer nanocontainer platform. *J. Cont. Release*. 2005; 102:475–88.

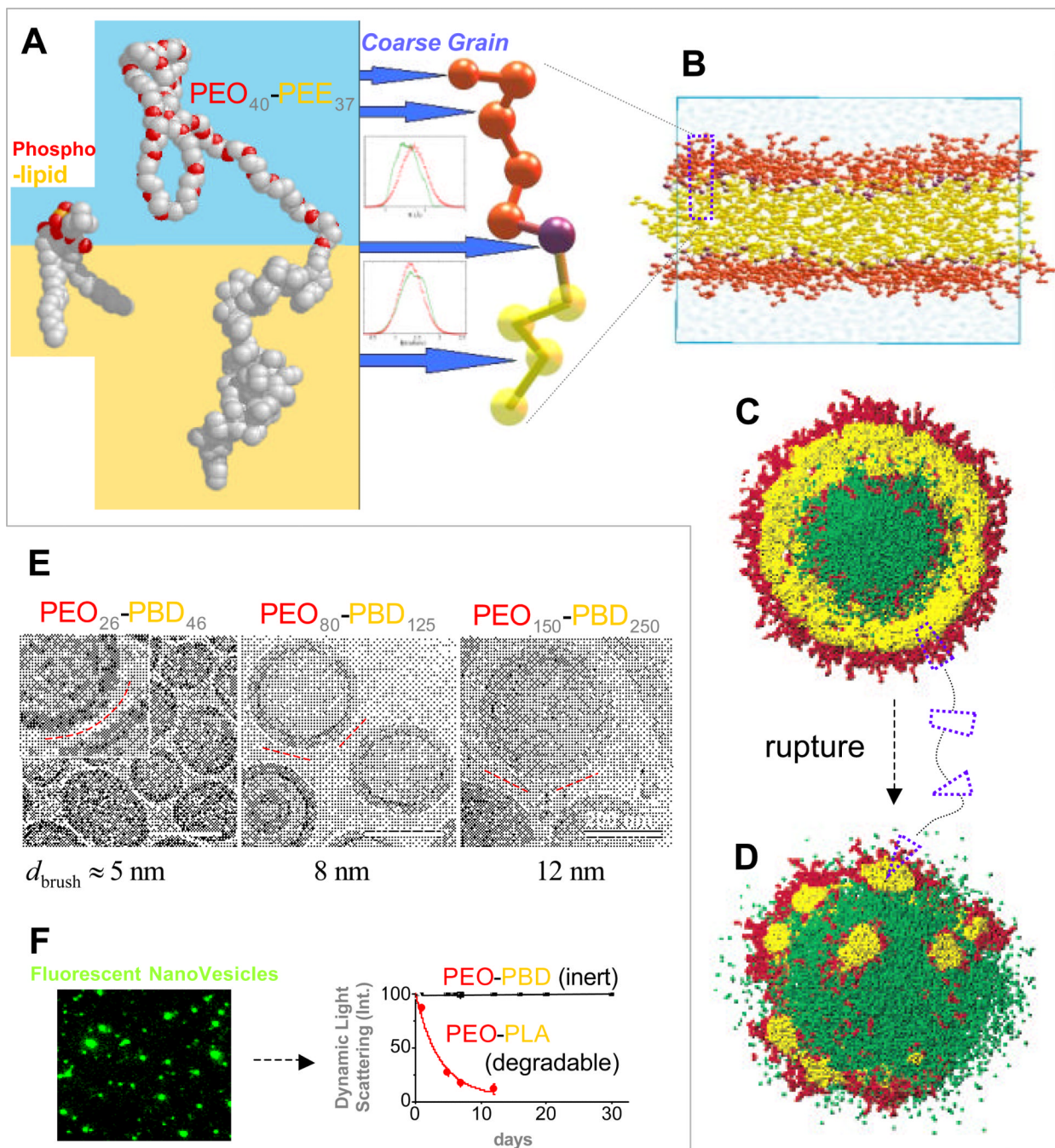


**Figure 1.** Polymersome assembly and disassembly by computer simulation and in experiment. (A) Atomistic representation of lipid (left) and amphiphilic diblock copolymer (right) and the potential-matching scheme used to derive an accurate coarse-grain model. (B) Membrane assembly of the coarse grain polymer within a periodic box of water. (C) Polymer nano-vesicle assembly simulated by dissipative particle dynamics using a simplified coarse grain polymer that allows larger scale simulations, including (D) disassembly and release of encapsulants. (E) Molecular weight series of diblock copolymer polymersomes imaged by cryo-TEM, which allows visualization of the hydrophobic core of PBD. The thickness of the hydrated and invisible PEO brush,  $d_{\text{brush}}$ , is estimated by measuring the closest distance

between adjacent vesicles and dividing by two. (F) Fluorescently labeled 100 nm nano-vesicles after dilution can be visualized as small dots by fluorescence microscopy. Dynamic Light Scattering provides an accurate measurement of vesicle size and, after periodic measurements, shows that PEO-PBD polymersomes are stable whereas vesicles composed with the degradable copolymer PEO-PLA disassemble over a period of days at room temperature.

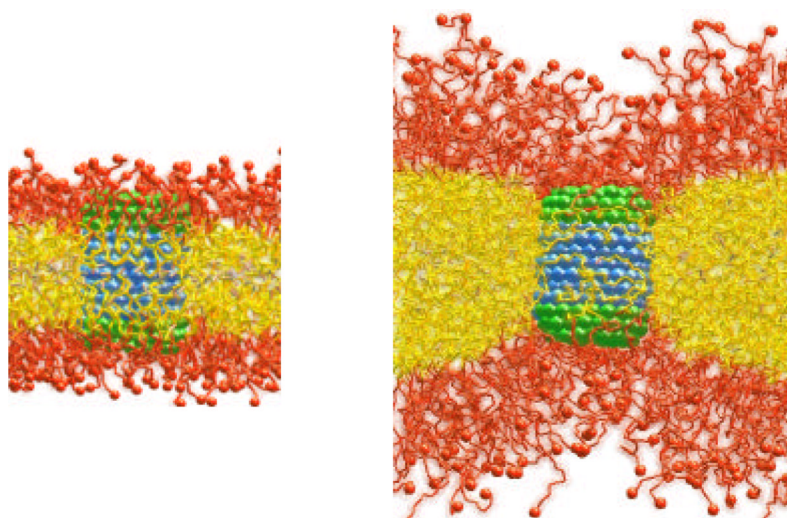


**Figure 2.** Stable insertion of a mimetic protein pore into either thin or thick block copolymer membranes, using coarse grain simulation methods. In the thicker membrane, polymer chains are sufficiently flexible to deform and accommodate the pore.



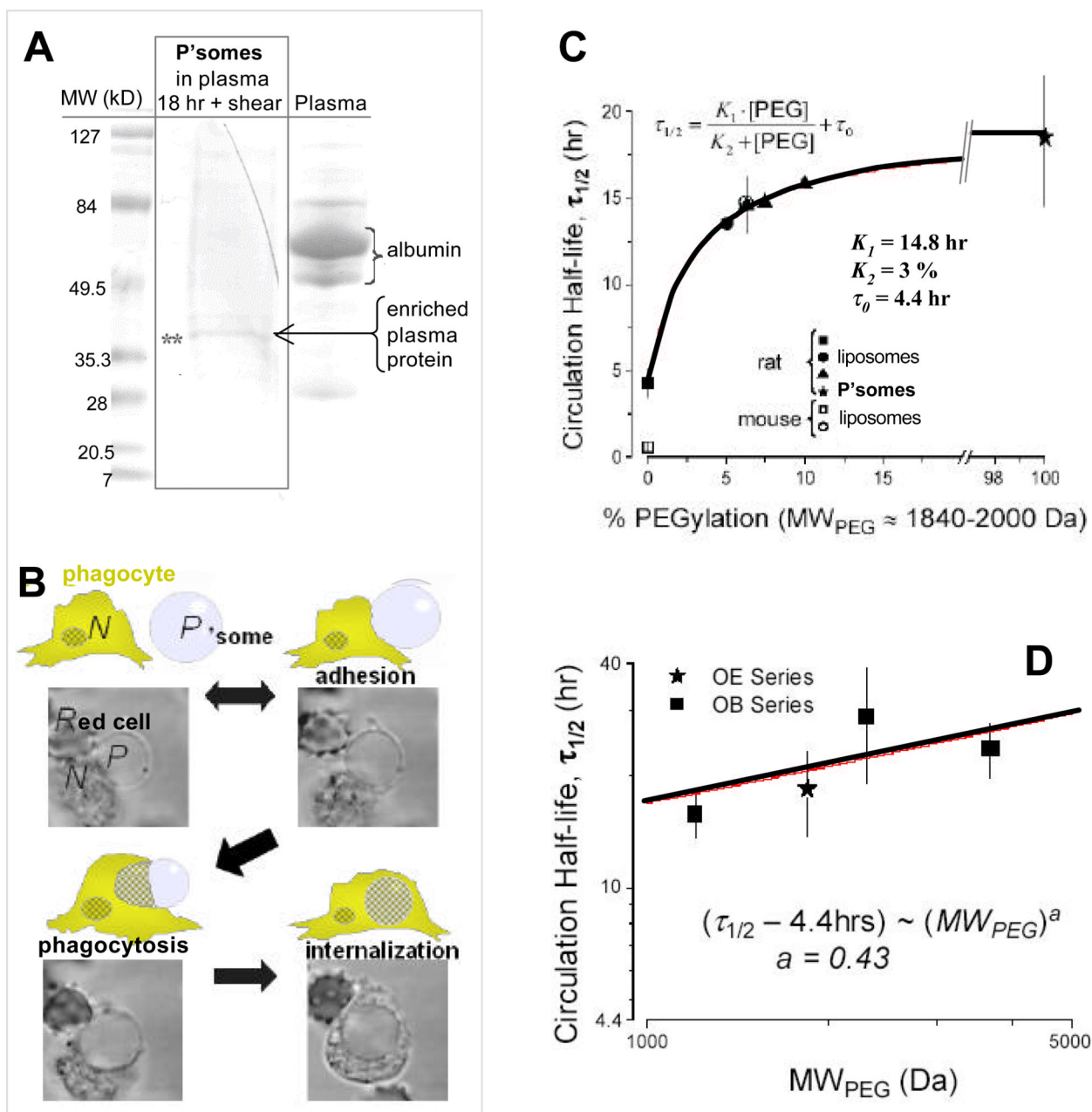


**Figure 3.** Polymersome interactions in the circulation. (A) Electrophoretic analysis of plasma proteins adsorbed to polymersomes incubated in blood plasma shows that select proteins interact with polymersomes and are enriched after 18 h, despite a hydrated PEO (or PEG) brush. Albumin is not detectable, but a protein around 40 kD is detected after separation of the polymersomes by centrifugation followed by vesicle solubilization with detergent. (B) Plasma-incubated polymersomes, *P*, will adhere to blood neutrophils, *N*, that will eventually engulf or ‘phagocytose’ such vesicles, leading to complete internalization. Adjacent red cells, *R*, do not adhere or interact with *N* or *P*. (C) Polymersomes have a 100% PEG brush, which can far exceed the PEG covering of PEGylated-liposomes, but the molecular weight of the PEG can be similar. Injections of 100-nm polymersomes into rats thus allow the circulation half-life to be determined as a function of %PEGylation. This kinetic measure

accumulated from data in the literature fits to a simple binding isotherm, suggestive of inhibition with an inhibition constant  $K_2$  as calculated. (D) For polymersomes with 100% PEGylations, the circulation time in rats increases weakly with the number-average molecular weight of PEG. The scaling exponent is close to that estimated for the PEG brush thickness.

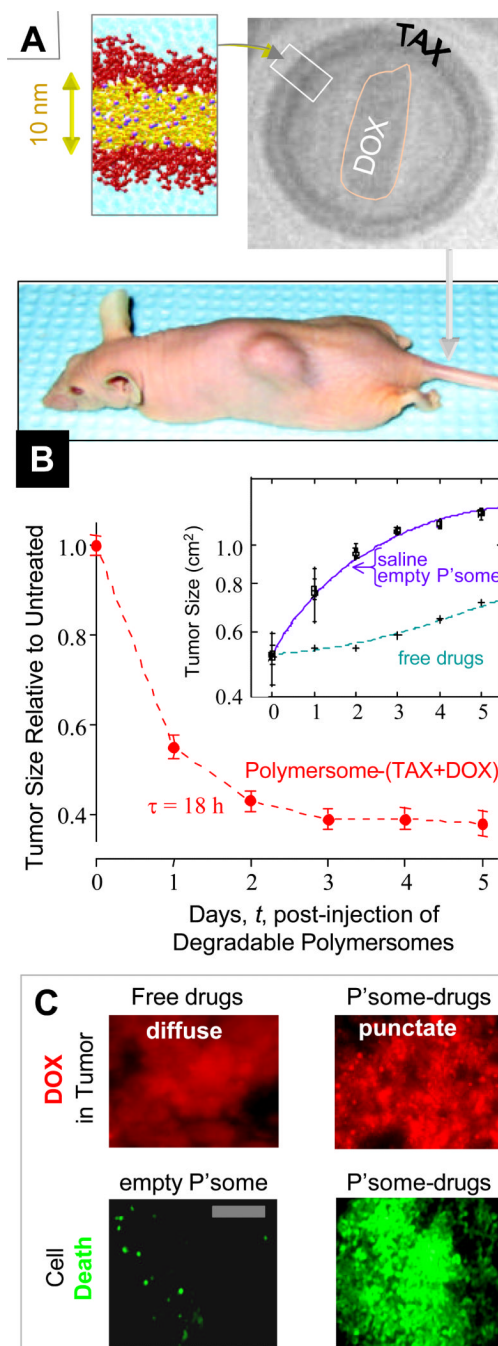


**Figure 4.** Dual drug-loaded degradable polymersomes shrink tumors. (A) Degradable polymersomes composed with PEG-PLA possess a membrane core that can be loaded with hydrophobic paclitaxel (TAX) and, within the interior, soluble doxorubicin (DOX) as a second anti-cancer drug. The latter is shown in cryo-TEM to precipitate or crystallize. The simulation snapshot at left illustrates the thickness of the hydrophobic core, which is about 3 times thicker than the core of a lipid vesicle and so polymersome membranes can carry more TAX. (B) Injection of these dual drug nano-carriers into mice bearing tumors of human-derived breast cancer cells shows rapid shrinkage of the tumor. The inset plot shows that empty polymersomes have no effect on tumor size when compared to saline injections; in

addition, injection of free drugs only slows tumor growth initially. (C) Imaging of tumor sections after 1 day allows DOX, which is fluorescent, to be visualized within the tumors. Delivery of free drug invariably shows diffuse staining of the tumors, whereas delivery of P'some-drugs leads to punctate images that suggest localization of the carriers to the tumors. Consistent with localization and tumor shrinkage, the drug-laden polymersomes induce massive cell death based on positive staining for apoptosis (TUNEL method).

**Table 1**

Assembled morphologies in water for PEO<sub>m</sub>-PEE<sub>n</sub> as determined in coarse grain molecular dynamics simulation [17].

<b>copolymer</b>	<b><math>f_{EO}</math></b>	<b><math>M_n</math></b>	<b>morphology</b>
EO <sub>21</sub> EE <sub>37</sub>	31%	3.0 kD	bilayer
EO <sub>73</sub> EE <sub>71</sub>	44%	7.3 kD	bilayer
EO <sub>50</sub> EE <sub>37</sub>	51%	4.4 kD	worm micelle
EO <sub>92</sub> EE <sub>37</sub>	66%	6.2 kD	spherical micelle